

## Generation of Synthetic SAS Data for Targets near the Seafloor: Propagation Component

Steven G. Kargl  
Applied Physics Laboratory, University of Washington  
1013 NE 40<sup>th</sup> St.  
Seattle WA 98105-6698  
Phone: (206) 685-4677 FAX: (206) 543-6785 Email: [kargl@apl.washington.edu](mailto:kargl@apl.washington.edu)

Award Number: N00014-10-1-0114  
<http://www.apl.washington.edu/projects/projects.php>

### LONG-TERM GOALS

In the final year of this project, the primary objective was the application of the propagation model to synthetic aperture sonar simulations and simulations for scattering within a homogeneous waveguide. Refinements to image source enumeration were implemented to ensure that time-of-flight wave packets, associated with an image source, arrive at a receiver location within a time window of interest.

### OBJECTIVES

The wave propagation model developed during FY11-12 was applied to several scattering problems, which included both waveguide simulations (i.e., reflections from upper and lower boundaries) and reduced half-space simulations (i.e., only interactions with a water-sediment interface). For the scattering problems, there are two wave propagation processes: (1) propagation from an image source to a target location, and (2) propagation from the target location to an image receiver. During step (1), the target location acts as a virtual receiver, and after the scattering process the target location becomes a virtual source. Thus, the refinement to the image source enumeration applies to the image receiver enumeration.

### APPROACH

A ray-base model developed in FY11 assumed a homogeneous layer of water between an upper semi-infinite half-space of air and a lower semi-infinite half-space of a homogeneous sediment. Rays are assumed to travel in straight line segments from a source location to a target location and after interacting with the target to a receiver location. Within the current report, the model is restricted to the propagation from an image source to a target location (i.e., a virtual receiver). For an interaction of a ray with an interface, an appropriate reflection coefficient is included in the received signal. At present the sediment can be modeled as either an attenuating fluid with a frequency-independent loss parameter or an effective density fluid model. For an image source located at  $\mathbf{r}_i$  and a target located at  $\mathbf{r}_t$ , the horizontal and total separation distances are  $|\mathbf{R}_t - \mathbf{R}_i|$  and  $|\mathbf{r}_t - \mathbf{r}_i|$ , respectively. The contribution of the  $i$ th source to the frequency spectrum at the target can be written as

$$P_i(\omega) = P_{src}(\omega)r_0 \left[ A^n(\theta_i)B^m(\theta_i) \frac{\exp(i\omega t_i)}{|\vec{r}_t - \vec{r}_i|} \right], \quad (1)$$

where  $P_{src}(\omega)$  is the frequency spectrum of the transmitted wave packet and  $r_0$  is a reference distance used in the calibration of the source level. The quantity within the square brackets accounts for the propagation of the ray. The reflection coefficients at the upper and lower boundaries are  $A(\theta_i)$  and  $B(\theta_i)$ . The local grazing angle  $\theta_i$  at a boundary is given by  $\cos(\theta_i) = |\mathbf{R}_t - \mathbf{R}_i| / |\mathbf{r}_t - \mathbf{r}_i|$ , and the  $m$  and  $n$  exponents indicate the number of interactions a ray has with a given boundary. The time delay for propagation from the source to the target is  $t_i = |\mathbf{r}_t - \mathbf{r}_i|/c$ . Here,  $c$  is the speed of sound in the waveguide. If the scattering from the target to the  $j$ th receiver were to be simulated, then Eq. (1) would be multiplied by the target's free-field scattering amplitude  $f(\theta_{ij}, \phi_{ij}, \omega)$  and a second factor similar to the quantity in the square brackets with  $t \rightarrow j$  and  $i \rightarrow t$ . The target-centered polar and azimuthal angles,  $\theta_{ij}$  and  $\phi_{ij}$ , are related to the local grazing angles  $\theta_i$  and  $\theta_j$ .

## WORK COMPLETED

During FY13, simulations of scattering from a 15-m radius fluid sphere in a 4000-m deep waveguide with source/receiver/target separation distances on the order of 100 km revealed the implementation of Eq. (1) violated reciprocity under certain conditions. If the source and receiver were located below the mid-depth of the waveguide the implementation satisfied reciprocity. If, however, either the source location or receiver location or both locations were above the mid-depth of the waveguide then reciprocity failed.

The failure was caused by a change in the enumeration of image sources, the method used to determine the reflection coefficient exponents, and the selection of image sources that contribute within a time window of interest. The depth of the waveguide is  $h$ , and the actual source is located at  $z_s$  ( $> 0$ ) with the water-sediment boundary at  $z = 0$ . Previously, the first image source in a set of image sources was placed below the water-sediment boundary with  $z_1 = -z_s$ , and the  $q$ th quartet of image sources was added to the set of image sources with the following  $z$ -coordinates:  $2qh + z_s$ ,  $2qh - z_s$ ,  $-2qh - z_s$ , and  $-2qh + z_s$  with  $q = 1, 2, 3, \dots$ . The initial ordering assumed that  $z_s < h/2$ , and the determination of the reflection coefficients assumed that the ray associated with the first image source always interacted with the lower boundary and the rays in the enumeration of the remaining image source then alternated with interacting with the upper and lower boundaries, respectively. As long as  $z_s < h/2$ ,  $z_1 = -z_s$ , and the addition of quartets followed the prescribed ordering, then the image sources were sorted in a manner consistent with the determination of the  $m$  and  $n$  exponents in Eq. (1), and reciprocity was ensured.

In the FY13 simulations with separation distances on the order of 100 km, it was advantageous to consider only a finite length time window with a defined time offset. It then followed that only image sources with propagation delays  $t_i = |\mathbf{r}_t - \mathbf{r}_i|/c$  within the time window needed to be considered; and so, the set of image sources were sorted by separation distances. When  $z_s > h/2$ , the new sorting led to a first image source with  $z_1 = 2h - z_s$ , and the ray associated with it reflects initially from the air-water interface. The implementation of the new model failed to updated the determination of  $m$  and  $n$ , and thus, reciprocity was violated.

## RESULTS

As an example to demonstrate that reciprocity holds for Eq. (1), a wave packet with a 10 Hz carrier frequency, 6 ms duration and Gaussian envelope was propagated from a source to a receiver in an homogenous water waveguide. The water depth was 4000 m with a sound speed and density of  $c_1 = 1500$  m/s and  $\rho_1 = 1000$  kg/m<sup>3</sup>. The sediment properties were  $c_2 = 1600$  m/s,  $\rho_2 = 2000$  kg/m<sup>3</sup>, and  $\delta =$

0.003 with  $\delta$  being the loss parameter. The source and receiver were initially placed at  $(0, 0, 1)$  and  $(0, 100, 1)$  with units of km. As a comparison, the wave packet was propagated by the ray model of Eq. (1) and a model based on the trapped modes in a waveguide. Figure 1a and 1b show the case where the source and receiver are below the mid-depth and Figures 1c and 1d show the case where the source (receiver) is below the mid-depth and the receiver (source) is above.

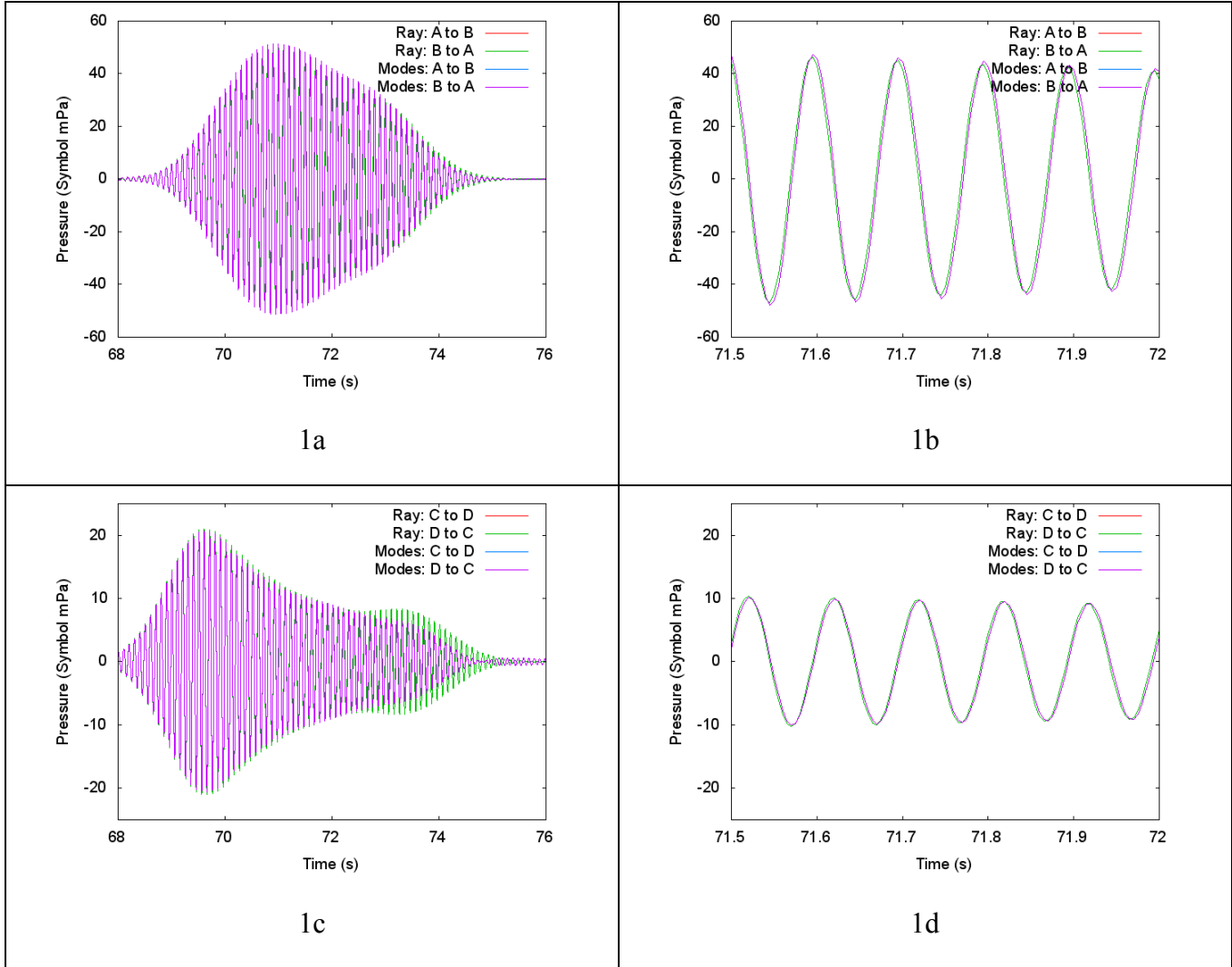


**Figure 1: (a) Propagation for a source (receiver) and a receiver (source) below the mid-depth. (b) Close-up of propagated signal in (a) demonstrating reciprocity. (c) Propagation for a source (receiver) below the mid-depth and a receiver (source) above the mid-depth. (d) Close-up of propagated signal in (c) demonstrating reciprocity. The location of the points are  $A = (0,0,1)$  km,  $B = (0,100,1)$  km,  $C = (0, 0, 1)$  km, and  $D = (0, 100, 3)$  km. Note, the red and green curves overlap and the blue and purple curves overlap.**

The discrepancy between the ray model and trapped mode model has been traced to an unphysical discontinuity in the frequency of the Green's function generated with the trapped modes model. The cause of this discontinuity is currently unknown.

## **RELATED PROJECTS**

The companion award (N00014-07-G-0557, Task 0023), “Generation of Synthetic SAS Data for Targets near the Seafloor: Target Scattering Component,” seeks to improve scattering models for targets near an interface used in SAS-ST. Improvements to the propagation model enhance the combined propagation and target scattering model.

The results of this project has been combined with the target scattering component and used as benchmark for the DARPA project, “Exploiting Seismic Events to Maintain Under-Ice Awareness,” (Award Number W911QX-12-C-0163). The project has developed a scattering model, based on the trapped modes in an inhomogeneous waveguide.

The research of this project in combination with the target scattering component has been used extensively in data-model comparison for the ONR funded project, “Acoustic Color of Mines and Mine-like Objects,” (N00014-07-G-0557/0032). It provides a fast robust model for the simulation of target scattering near and at an interface.